J. Mar. Biol. Ass. U.K. (2007), **87**, 47–58
Printed in the United Kingdom
doi: 10.1017/S0025315407054951

On the possibility of detecting surfacing sperm whales at risk of collision using others' foraging clicks

E. Delory*, M. André*‡, J.-L. Navarro Mesa† and M. van der Schaar*

*Laboratori d'Aplicacions Bioacústiques, Escola Politècnica Superior d'Enginyeria de Vilanova i la Geltrú, Universitat Politècnica de Catalunya, Spain. †Departamento de Señales y Comunicaciones, Universidad de Las Palmas de Gran Canaria, Spain. ‡Corresponding author, e-mail: michel.andre@upc.edu

Cetaceans are prone to collisions with fast vessels, and in areas of high cetacean and vessel density such as in the Canary Islands, the sperm whale (*Physeter macrocephalus*) is of great concern. Sperm whales are highly vocal and can be localized with passive sonar, but, when at or near the surface, they tend to stop vocalizing, i.e. when they are most at risk. Regrettably, ship-borne active solutions have proven inefficient due to the short detection range and the ships' high-speeds. Our objective in this paper is to evaluate the efficiency of an original passive sonar solution that would use vocalizing whale clicks at depth as acoustic sources to detect silent whales. This solution could be a non-invasive complementary component of a more complex passive localization whale anti-collision system. To meet this aim, a simulation tool for 3D acoustic propagation was designed in which a wideband Nx2D ray solution of the wave equation simulates a passive solution consisting of an arbitrary number of active acoustic sources, an illuminated object, and a receiver, all positioned in a three-dimensional space with arbitrary bathymetry. Both curved and straight ray solutions were implemented, the latter providing greater computational speeds at the expense of temporal and angular precision. The software recreates the resulting sound mixture of direct, reverberated and target back-scattered signals arriving at the array sensors for any array configuration, any number of sources and one target. Simulations show the application of the concept for the Canary Islands, with a detection range upper bound of the order of one kilometre.

INTRODUCTION

Sound propagates in water better than any other form of energy (Urick, 1996), thus cetaceans have adapted and evolved integrating sound in many vital functions such as feeding, communicating and sensing their environment. In areas where marine mammal monitoring is a concern, detection and localization can therefore be efficiently achieved by passive sonar, but provided that the whales are acoustically active. When near or at the surface, where they may remain for 9 to 15 min between dives (Gordon, 1987; Gordon & Steiner, 1992; André, 1997; Watwood et al., 2006), sperm whales (*Physeter macrocephalus*) are known to stop vocalizing (Jaquet et al., 2001). Not discarding the possibility of deploying static active sonar solutions that would scan the high-risk areas, the concern that whales are highly sensitive to anthropogenic sound sources (Richardson et al., 1995) has motivated the search for alternative passive means to localize them.

The whale anti-collision system (WACS) is a passive sonar system to be deployed along maritime routes where collisions are a concern for public safety and cetacean species conservation (André et al., 2004a,b; 2005). The WACS will integrate a three-dimensional localization passive array of hydrophones and a communication system to inform ships, in real-time, of the presence of cetaceans on their route. To detect silent whales, alternatives to conventional passive methods should be explored in order to avoid or complement active sonar support. In the present case, i.e. a group of sperm whales consisting of silent and vocal individuals, using the latter's highly energetic clicks might prove effective as illuminating sources to detect silently surfacing whales.

Ambient noise imaging (ANI) uses underwater sound just as terrestrial life forms use daylight to visually sense their environment. Instead of filtering the surrounding ocean background noise, ANI uses it as the illuminating source and searches the environment for a contrast created by an object underwater (Potter et al., 1994; Buckingham et al., 1996). Although ANI is fraught with technical difficulties and has been validated, to date, at relatively short ranges (Pallayil et al., 2003) it opens new insights into acoustic monitoring solutions that are neither passive nor active in the strict sense.

The solution introduced in this paper is conceptually based on both ANI and multi-static active solutions, where the active sources are produced by surrounding foraging sperm whales at greater depths (from 200 m downwards), which vocalize on their way down and at foraging depths (Zimmer et al., 2003), and in reported cases, likely on their way up until a few minutes before surfacing (Jaquet et al., 2001).

A comparable approach was introduced for the humpback whale (*Megaptera novaeangliae*) off eastern Australia (Makris & Cato, 1994; Makris et al., 1999). In this study, if the solution were to be applied for monitoring purposes, it would be difficult to implement due to the need for near real-time shallow water propagation modelling as humpback whale

vocalizations' spectra peaks are at rather low frequencies and as a result happen to be severely altered in the shallow water waveguide. This may prevent correct pattern matching between the direct and reflected signals unless accurate modelling techniques are applied. Comparatively, sperm whales' vocalizations spectra are considerably wider, higher in frequency, and of greater intensity. Their transient nature also makes received signals less prone to overlaps. Furthermore, our interest is in the propagation of these clicks in deep water and at relatively shorter distances, where the wave propagation problem is more tractable than for shallow water and long distances. These differing characteristics motivated us to revisit this passive approach and test the efficiency of using deep diving sperm whale clicks as a source to illuminate silent whales near the surface.

Amongst numerous constraints, a prerequisite for sperm whale clicks to be used as active sources is that acoustically active whales should be close and numerous enough to create a repeated detectable echo from silent whales. The chorus created by these active whales should occur day and night and possibly all year long. Hence the following demonstration relies on the condition that whales are foraging in a group spread over not more than a few square kilometres and where a substantial amount of them are present within that range. Such a scenario has been observed consistently in the Canary Islands (André, 1997) and in the South Pacific (Jaquet, 1996; Jaquet & Whitehead, 1996), where sperm whales tend to travel and forage in groups of around ten adults, mostly female, spread over several kilometre distances with a separation on the order of one kilometre between individuals.

In addition to the above, a substantial amount of information on temporal, spectral and directional aspects of the sources is essential. Time–frequency content of sperm whale clicks, their level and directionality have been investigated (Goold & Jones, 1995), and are reviewed in the following sections.

In order to evaluate the possibility of detecting and localizing silent whales near the surface using other conspecifics' acoustic energy, a considerable amount of information on sperm whale acoustics was analysed and computed to create a simulation framework that could recreate a real-world scenario.

Amongst other modules, a piston model for the generation of clicks is described that accounts for the data available to date. The modelled beam pattern supports the assumption that sperm whale clicks may be good candidates as background active sources. A sperm whale target strength (TS) model is also introduced that interpolates the sparse data available for large whales in the literature. Sperm whales' typical spatial organizations, acoustic behaviour, as well as the known patterns of click time-series are reviewed and parameterized.

3D MODELLING OF THE SPERM WHALE CLICK BEAM PATTERN

Our objective is to create a three-dimensional broadband model of a sperm whale click beam pattern to simulate the applicability of sperm whale clicks as usable active sources. Accordingly, a synthesis of known available data on click sound pressure level, time–frequency distribution and directionality is presented. As a result a 3D model of the sperm whale click beam pattern is created.

Sperm whale acoustics

Research on the acoustic features of sperm whale clicks is well documented, but the obtained quantitative results have varied substantially between publications. Only recently have the intricate sound production mechanisms been addressed with reliable quantitative data (Møhl et al., 2000; Zimmer et al., 2005a,b).

Source level and directionality

In 1980 Watkins reported a source level (SL) of 180 dB *re* 1µPa-m and suggested that clicks were rather omni-directional (Watkins, 1980), whereas recent results from Møhl et al. estimate this source level to be as high as 223 dB_{peRMS} *re* 1µPa-m with high directionality (Møhl et al., 2000, 2003). Morphophysiological observations by Norris & Harvey (1972) on the unusual shape and weight of the sperm whale nose are in clear agreement with the hypothesis of its highly directional and powerful sonar function, supported by Møhl's results.

Goold & Jones (1995) recorded clicks from both an adult male and female and measured a shift to higher frequencies of the main spectral peaks, from 400 Hz to 1.2 kHz, and 2 kHz to 3 kHz, though they noticed that this shift was rather unstable. Spectral contents of clicks as a function of body size and, most importantly, animal orientation information could help to explain this difference in received levels. The almost ubiquitous lack of animal heading information at click recording time in published material makes results hardly usable for a reliable 3D model. To date, Møhl et al. (2000, 2003) and Zimmer et al. (2005a) are the only studies that provide sufficient calibrated material to produce a correct model. The reported 15 kHz centroïd frequency and apparent source levels higher than 220 dB_{RMS} *re* 1µPa-m corroborate the fact that most previously published click levels and characteristics certainly stemmed from off-axis recordings or unsuitable recording bandwidth.

Sperm whale click source level and time–frequency characteristics can be predicted by inferring a three-dimensional model, which is based upon well-known physics principles, such as the direct relationship between the size of the sound production apparatus and its directionality (Tucker & Glazey, 1966).

In our model we infer that sperm whale click spectra are exclusively related to body length, though regardless of the age and sexual dimorphisms established by Cranford (1999) and Nishiwaki et al. (1963), as no data to date allow for proper physical connections between these morphophysiological discrepancies and the clicks' 3D characteristics. Previous reports on smaller odontocetes have demonstrated that species of smaller size tend to emit higher peak frequencies compared to sperm whales, whereas on-axis source levels over 210 $dB_{p\text{-}p}$ *re* 1µPa @ 1m are consistently reported (Au & Herzing, 1997, 2003; Philips et al., 2003; Rasmussen et al., 2002). Short of proper directional data to rely upon for females, we conjecture that female sperm whales follow the same rule, with on-axis levels equivalent to males but with a size-related up-shifted spectrum and shorter duration,

https://doi.org/10.1017/S0025315407054951 Published online by Cambridge University Press

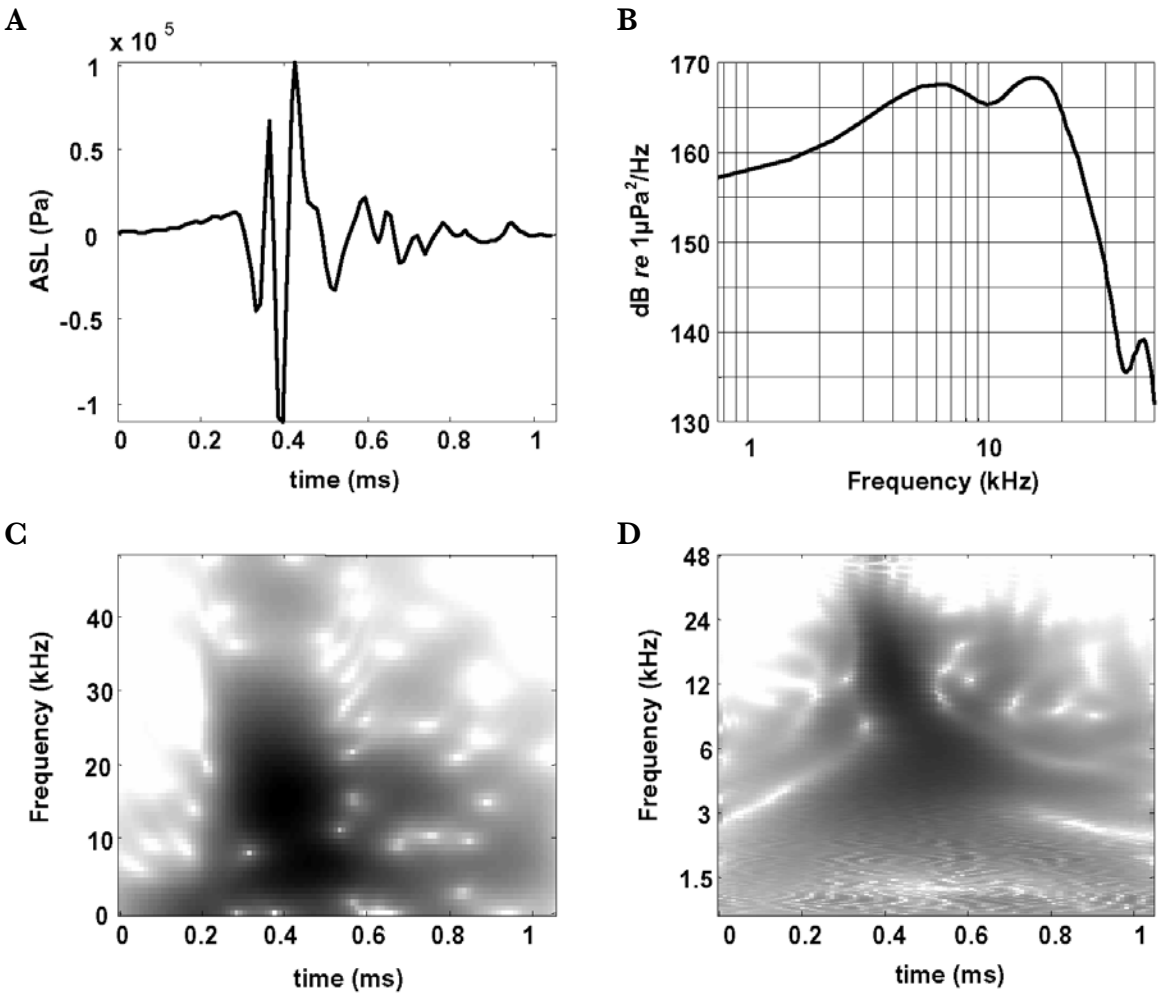

Figure 1. This monopulse click was recorded near on-axis from an adult sperm whale off Andenes (B. Møhl et al., 2003). Sampling rate is 96 kHz. (A) Waveform, apparent source level in µ*P*a; (B) the received power spectral density by averaged periodogram, continuously on 32-sample windows, Hamming weighted; (C) continuous spectrogram, Hanning weighted, calculated on 128 pts-zero-padded FFT windows of 32 samples; (D) click scalogram by Meyer continuous wavelet transform envelope. (C) and (D) greyscales span 180–230 dB *re* 1µPa^2/Hz, apparent source level.

which actually results in lower energy flux density but equal intensity.

Click time–frequency characteristics

Acoustic recordings of distant sperm whales have often revealed the multi-pulsed nature of their clicks, with inter-pulse intervals that may be related to head size or more specifically the distance between the frontal and distal air sacs situated at both ends of the spermaceti organ (Alder-Frenchel, 1980; Goold, 1996; Gordon, 1991; Møhl et al., 1981; Møhl & Amundin, 1991). While the utility of this multi-pulsed pattern is unclear, Møhl et al. (2003) have shown that one single main pulse appears for on-axis recordings. They suggest that the radiated secondary pulses are acoustic clutter resulting from the on-axis main pulse generation. This clearly advocates that the animal orientation must be known in order to create a 3D click time–frequency model from recorded sound.

These multiple pulses are found in the upper half of the received click spectrum while on-axis recordings reveal a centroïd frequency of 15 kHz and a monopulse pattern (Figure 1). On recordings we performed in the Canary Islands from whales of unknown orientation, more than six secondary pulses could at times be observed. A continuous low frequency part (below 1 kHz), which does not seem to follow a repetitive pattern and may last more than 10 ms, has also been documented (Goold & Jones, 1995; Zimmer et al., 2003).

Proper time–frequency modelling from recorded clicks should therefore account for animal instantaneous distance, heading and depth, and environmental conditions with sufficient space–time resolution. To our knowledge, no other report fulfils these requirements. Yet, our aim here is not to model an even near-perfect click generator, but a system that is in agreement with our current knowledge.

Temporal patterns of click series

Sperm whale clicks were also chosen as a possible source for this work for the known steadiness of the click production rates. The obvious advantage is the possibility for the monitoring system to search the environment for steady and coherent responses, as a means of raising the detection thresholds and, as a result, reducing false alarm rates.

https://doi.org/10.1017/S0025315407054951 Published online by Cambridge University Press

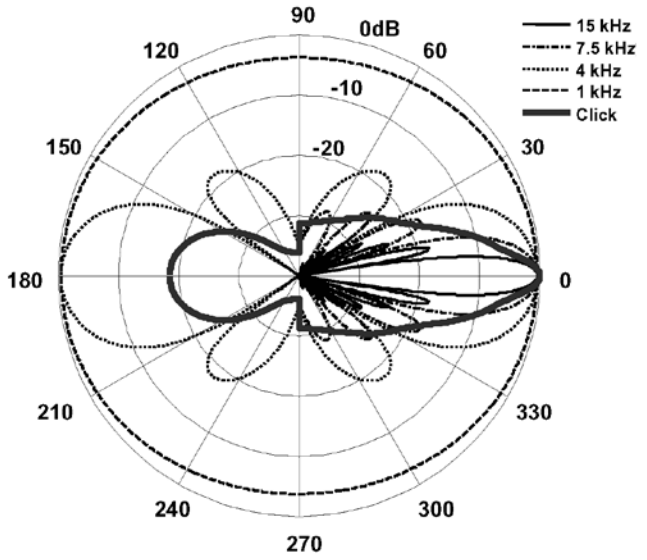

Figure 2. Composite beam pattern of the click created by applying its estimated power spectral density to a 0.8 m circular transducer that creates forward beams only from 3.5 kHz upwards, and bidirectional beams downwards. The resulting click DI is 22,3 dB. See text.

Sperm whale clicks are mostly sequential and inter-click-intervals (ICIs) rarely exceed 5 s. Most commonly encountered are the so-called 'usual clicks', which are produced a few seconds after the feeding dive starts and end a few minutes before surfacing (Gordon & Steiner, 1992; Jaquet et al., 2001; Douglas et al., 2005). ICIs of usual clicks span 0.5 to 2 s. Clicks of ICI lower than 0.1 s are called rapid clicks, and those of ICI higher than a few seconds are called slow clicks (Watkins, 1980; Gordon, 1987; Weilgart & Whitehead, 1988). Creaks are series of clicks with a much higher repetition rate, as high as 200 s^{-1}, and are believed to be used for sonar and foraging exclusively. Sperm whales are also known to produce 'codas', defined as short sequences (1–2 s) of clicks of irregular but geographically stereotyped ICIs (Pavan et al., 2000; Watkins & Schevill, 1977; Weilgart & Whitehead, 1993). A more elaborate form of ICI analysis performed on usual clicks showed that the ICI may follow a rhythmic pattern that could be used as a signature by individuals of the same group. This pattern is a frequency modulation of the click repetition rate of usual clicks (André & Kamminga, 2000).

In view of the above summary, the essential information is that we can rely upon a high click repetition rate that may generate better estimates in a short time period. We believe that simulations that would implement all known types of click temporal patterns would probably not add significant information at this phase of the study.

Consequently, our demonstration will contemplate usual clicks only. As a result, in a simulation where a given group of sperm whales are clicking in chorus, each individual will be assigned an ICI sampled from a uniform probability density function on the [0.5;2] second interval.

3D modelling of the sperm whale sonar click

The unusual content and shape of the sperm whale nose has led to various hypotheses on the biophysical processes involved in click production. Norris & Harvey (1972) suggested a single tube able to generate multi-pulsed sounds, and Møhl et al. (2001, 2003) updated this theory with the analogy 'that sees the spermaceti organ and junk compartment as two connected tubes, forming a bent, conical horn'. In addition, a flat circular piston model was shown to match an adult male click beam pattern in azimuth (Møhl et al., 2003; Beedholm & Mohl, 2006). Interestingly, the matching piston had an 80 cm diameter, which corresponded to the diameter of the frontal air sac that had been reported for adult male sperm whales in the same area. For comparison, Au et al. (1986) could match an Atlantic bottlenose dolphin beam pattern with a flat circular 8 cm diameter piston. The latter and the observation that a sperm whale click radiation pattern could well be linked to its frontal sac size prompted us to make the 3D beam pattern a function of body size, so that the piston model could be proportionally downsized for females from adult male data. The piston model is further adapted so that low and high frequencies are treated differently, in closer agreement with what is known of the animal anatomy and the click dominant frequencies when these are recorded off-axis. In view of the above, we anticipate that:

1. The parabolically shaped skull acts as a reflector that greatly contributes to the coherent addition of direct and skull-reflected high frequency waves ahead of the animal. The skull-only contribution to forward beams has been demonstrated for the common dolphin (*Delphinus delphis*) in (Aroyan, 1996), the results of which are extrapolated here to the sperm whale and applied to the piston model. This further implies that a limit frequency in relation to the skull size should be set, under which the coherent forward beam creation hypothesis no longer stands.
2. This cut-off frequency is approximately 3 kHz for males, as suggested in Zimmer et al. (2005a).

To adapt the piston model to the above hypotheses, the set of equations for the far-field, on-axis normalized, rotationally symmetric radiation pattern we anticipate are:

$$\begin{aligned} D_{ka>2}(\theta) &= \frac{2\mathcal{J}_1(|ka\sin(\theta)|)}{|ka\sin(\theta)|} \quad \theta \in [-\pi/2, \pi/2] \bmod 2\pi \\ D_{ka>2}(\theta) &= 0 \quad \theta \in]\pi/2, 3\pi/2[\bmod 2\pi \\ D_{ka\leq 2}(\theta) &= \frac{2\mathcal{J}_1(|ka\sin(\theta)|)}{|ka\sin(\theta)|} \quad \theta \in \Re \end{aligned} \tag{1}$$

where θ is the angle to the whale head axis, k the wavenumber, a the piston radius, and $\mathcal{J}_1$ the order 1 Bessel function. The interval [-π/2:π/2] stands for the frontal half-space, and click propagation towards the back of the animal only occurs at frequencies <3 kHz. The resulting beam pattern for the near on-axis click in Figure1 from a 14 m sperm whale is plotted in Figure 2.

SPERM WHALE TARGET STRENGTH

There are few records of target strength (TS) measurements of marine mammals; this lack of information follows from the early whaling industry relying only on visual cues to localize whales. In addition, the need for marine mammal

https://doi.org/10.1017/S0025315407054951 Published online by Cambridge University Press

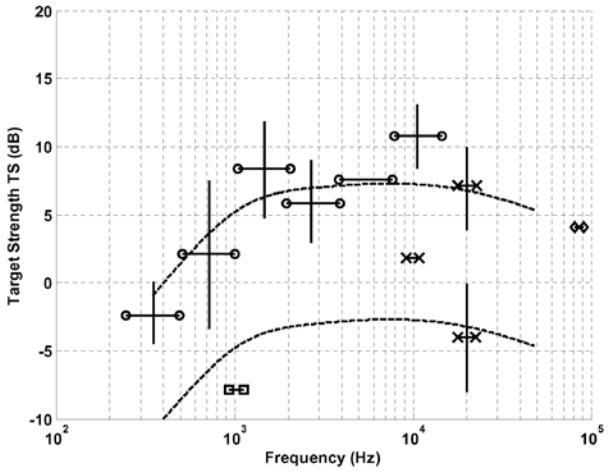

Figure 3. Sperm whale target strength interpolation from field measurements on sperm whale, humpback whale and right whale. Vertical lines show the measurement's standard deviation. Horizontal lines are the measurement bandwidths and symbols account for data source: circle, square, cross and diamond are Levenson, Dunn, Love and Miller respectively. Interpolation curves result from smoothing splines with an average of 1 dB tolerance at each knot, top and bottom curves stand for TS beam and beam ±45° aspect respectively.

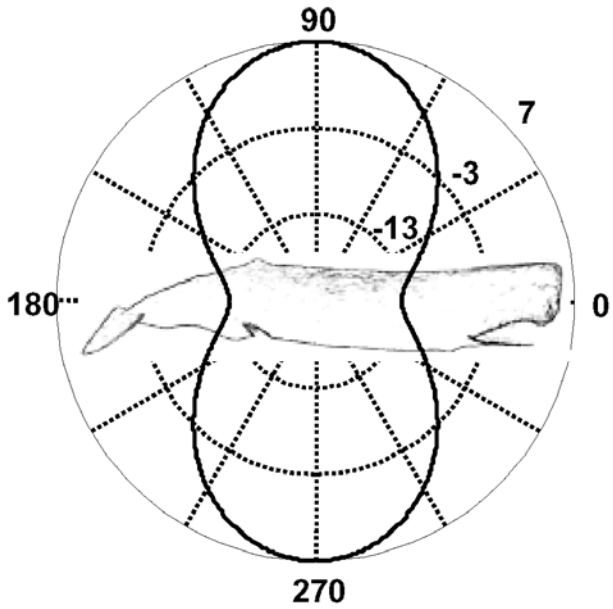

Figure 4. Sperm whale target strength values in dB, function of aspect angle to the source at 3 kHz for a 10 to 15 m adult. The model is assumed invariant by rotation around the 0° axis. The polar pattern results from the evaluation of equation 2 at the TS value obtained from smoothing spline interpolation at 3 kHz.

TS measurements for conservation and research purposes is only very recent.

Dunn (1969) reported a measured TS of –8 dB for one sperm whale in the 1/3rd octave band centred at 1.0 kHz but the aspect angle was unclear (although assumed to be from bow), while the author suggested that the beam aspect could raise TS to values as high as 10 dB. Interestingly, Love(1973) gave a head-on TS of –4 and beam aspect of 7 dB at 20 kHz for a 14 m humpback whale and a beam aspect TS of 2 dB at 10 kHz for a 9 m specimen. As both species grow to equivalent sizes we could expect them to be equally reflective to sound and possibly extrapolate, though keeping in mind that this extrapolation could be erroneous if blubber thickness and lung sizes greatly differed, as was stated by Miller et al. (1999a). Similarly, Levenson (1974) measured sperm whale bi-static TS average values of –2.5 dB in the 250–500 Hz band and 10.8 dB in the 8–16 kHz band, but could not demonstrate whether these values came from small pods or solitary animals, and no aspect angle information could be provided. More recently, TS measurements at 86.25 kHz were reported for a right whale and a humpback whale of the same size (15 m), and differences of 5 dB were attributed to differences in blubber thickness (Miller et al., 1999a,b; Miller & Potter, 2001). They measured a broadside TS of 4 dB for the humpback, and showed that the aspect angle could raise TS differences by at least 6 dB, in agreement with Love's results. High-frequency absorption in blubber was shown to be the most probable cause of lower TS in right whales compared to the humpback. A parallel to the sperm whale case can be drawn and we therefore expect that, as sperm whales are known to have thinner blubber than right whales, the right whale high-frequency TS measurement is not representative and should not be considered for extrapolation.

From the above measurements we created a composite plot (see Figure 3). Clearly, Levenson's TS results are offset to higher TS values, which may stem from the uncertainty about whether there was a single individual or several. Nonetheless, this graph highlights two characteristics: (1) bow or head aspect angle to the source reduces TS values substantially; and (2) TS values decrease with frequencies lower than 1 kHz and higher than 16 kHz. This is in agreement with the underlying physics: long wavelengths compared to target cross-section size reduce reflection, and absorption of frequencies above 20 kHz in whale blubber starts being significant, as was shown by Miller & Potter (2001).

It is important to note that the main resonant frequencies of whale lungs, which probably are the most reflective organs, are at least two orders of magnitude lower than the frequencies of interest here (Finneran, 2003). Thus, the possibility that a contributing resonant peak frequency may exist can reasonably be ruled out.

The stated measurement uncertainties and variability of the results make accurate modelling of the target strength as a function of frequency, orientation and animal size, an ambitious task. We first opted for interpolating the reported TS measurements using smoothing splines, for animals of size ranging from 10 to 15 m, for which data are available. We limit the bandwidth to 1–30 kHz, where sperm whale clicks are the most energetic and target strength values are supposedly highest. To account for the angle of incidence, an offset is applied to the interpolated beam-aspect TS function. In agreement with the above, a mono-static TS polar plot displaying the angle-dependent offset function is presented in Figure 4, the formulation of which is:

$$TS(f,\theta) \equiv -TS_0(f)\cdot\cos(2\theta) \qquad \theta \in \Re \qquad (2)$$

where θ is the animal aspect angle to the source and TS_0 is the

https://doi.org/10.1017/S0025315407054951 Published online by Cambridge University Press

Table 1. *Simulation settings.*

Parameters	
Working bandwidth	1000 to 30,000 Hz
Animals size/sex	10 m/female
Piston diameter	2/3 of 0.8m
On-axis click-level (0–48kHz)	220 dB*rms re* 1µPa@1m
Number of vocal whales	8
Minimum horizontal distance between vocal whales	1000 m
Depth of vocal whales	200 to 2000 m
Number of silent whales	1
Depth of silent whales	100 m
Simulation site	5 km square area half-way between Gran Canaria and Tenerife
Bottom reflection coefficient (intensity)	0.5
Wave height (m)	1
Velocity profile equation	Mackenzie

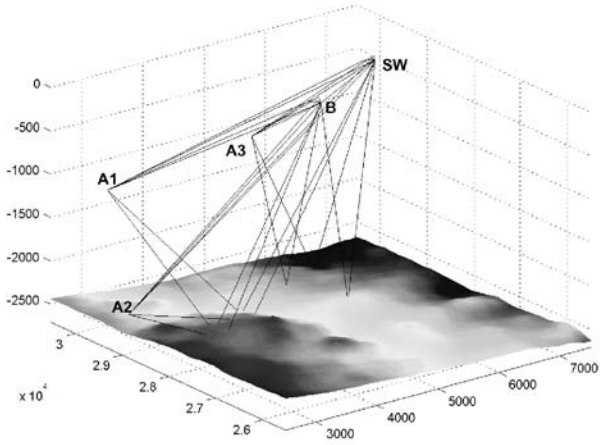

Figure 5. 3D representation of rays with bottom, surface and object reflections with varying bathymetry resulting from our simulation software *Songlines*. A1–3, 3 vocal whales; SW, silent whale at 100 m depth; B, monitoring buoy, here located half-way between Gran Canaria and Tenerife Island (km 28) on the maritime channel. Ray paths account for vocal whale to buoy, vocal whale to non-vocal whale, silent whale to buoy, and their respective bottom and surface reflection paths. All dimensions in metres.

frequency dependent beam-aspect TS function interpolated from reported data. The 3D TS function follows by rotation around the animal longitudinal axis.

SPERM WHALE ACOUSTIC BEHAVIOUR AND SPATIAL ORGANIZATION

Sperm whale sightings have been reported from all over the world (Jefferson et al., 1993). While males are known to travel to higher latitudes, females tend to remain under the 40° latitude. Apart from this sexual discrepancy, different types of groups may be found depending on the area. Off the Californian coast, three distinct associations can be found: (1) large mixed groups (10 to 50 individuals) consisting of young and adult females, juveniles and pubertal males; (2) groups of up to a dozen young adult males spreading over a 10 km square area; and (3) solitary old males up to 17 m long (Caldwell et al., 1966). In the Canary Islands, sperm whale groups are resident and generally consist of adult females and juveniles (mixed groups), while adult males travel alone from one group to another, implementing a reproductive 'searching strategy' (Best, 1979; André, 1997). Adult males are also known not to remain in the area and only appear during reproductive periods. According to André (1997), mixed groups consist of more than ten animals, a maximum of two kilometres apart and they keep distances of at least 500 m between individuals. Maintaining this spatial organization, the group travels at an average speed of 2 knots (with maxima of 4 to 10 knots in rare cases), alternating forty-minute dives often down to more than 800 m with 15-min rest periods at or near the surface. Deep whales keep on clicking while whales at or near the surface mostly remain silent, in agreement with Whitehead & Weilgart (1990) and Jaquet et al. (2001). This scenario was observed consistently throughout the field studies between 1993 and 1996 in the Canary Islands.

In this paper, we will focus on the mixed group association to simulate our passive approach. In the next section, we describe how this scenario is recreated.

MATERIALS AND METHODS

3D simulation of wave propagation from source-to-receiver and source-to-object-to-receiver in the bounded medium is implemented by software that we designed based on a ray tracing model. This well documented and thoroughly utilised method provides good approximation of the full wave equation solution when the wavelength is small compared to water depth and bathymetric features (Jensen et al., 2000). As seen above, whale TS and click spectra curves prompted our approach only for frequencies above 1 kHz, i.e. a 1.5 m wavelength, a value far smaller than any other physical scale in the problem.

Bathymetry and sound speed profile

Bathymetric data between the islands of Gran Canaria and Tenerife were obtained with a SIMRAD EM12 multibeam echo-sounder and provided by S. Krastel, University of Bremen, Germany. The bathymetric map horizontal resolution is 87 m (see Krastel & Schmincke, 2002 for details). Sound speed profile was estimated by salinity, temperature and pressure measurements up to 1000 m applied to Mackenzie's equation (Mackenzie, 1981), and from 1000 m to the ocean bottom (>3000 m at many locations) by linear extrapolation and increasing pressure, while considering temperature and salinity constant, because no deeper data were available to us. The resulting profile was close to typical North Atlantic sound speed profiles found in the literature (Urick, 1996).

Boundaries

The operating mechanisms at the surface and sea-floor boundaries are incorporated through their physical characteristics (Etter, 2003). Sea surface effects are limited to reflection loss, reflection angle and spectral filtering. Surface

https://doi.org/10.1017/S0025315407054951 Published online by Cambridge University Press

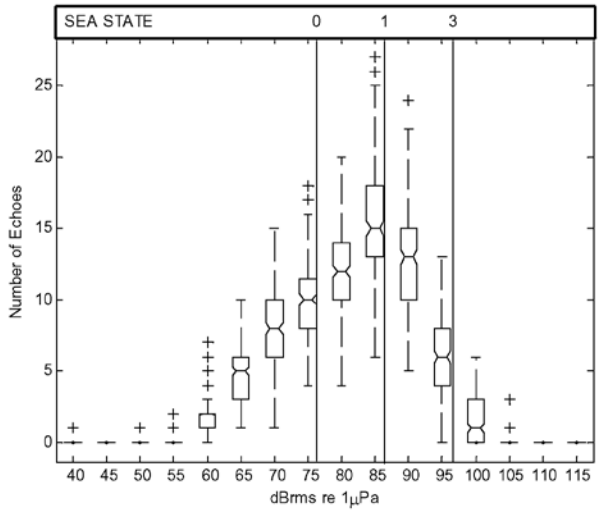

Figure 6. Statistical plot of the simulated received RMS levels of clicks reflected on a silent whale located at 1000m distance from the buoy (see text for details on simulation settings). Ordinates represent the median number of contributing clicks per simulation drawn from 200 simulations (each simulation includes 8 vocal whales clicking once). Also plotted are lines at the lower quartile and upper quartile values. The whiskers are lines extending from each end of the box to show the extent of the rest of the data. Outliers are data with values beyond the ends of the whiskers. Notches over and below median values are medians' 95% confidence intervals. Sea-states 0 to 3 and above noise levels in the 1-30 kHz bandwidth are represented (calculated from Urick, 1996).

reflection loss is estimated by the Rayleigh parameter, as a function of the acoustic wavelength and the root-mean-square amplitude of surface waves. Angles of reflection are determined by the Snell law, whereas neither surface nor bottom scattering are modelled. Sea-floor effects are limited to reflection loss and reflection angle.

Other parameters

An arbitrary number of acoustically active whales and one passive object defined by a 3D TS function can be arbitrarily positioned in the three dimensions. All active whales can be assigned a different and arbitrary waveform, the spectral information of which is estimated and affects the absorption parameter as well as the source radiation pattern. To test the efficiency of arbitrary hydrophone arrays, beamforming can be processed at the receiver location by mapping direction of arrival into phase delays and recreating the sound mixture at all sensors. To ease the implementation and testing of the ray solution, a graphical user interface was created under Matlab and called *Songlines*.

Implementation

We first delimit a 5 km×5 km square area around the monitoring point, located at 40 m depth, half-way between Tenerife and Gran Canaria islands (Canary Islands, Spain), where 8 clicking whales of 10 m size are pseudo-randomly positioned between a depth of 200 m and 2000 m, with the condition that animals maintain a minimum distance of 1 km between each other. One silent whale is at 100 m depth and at a controlled distance from the monitoring point of 1000 m. All whales travel in the same direction at a 2 knot horizontal speed and random elevation. Inter-click intervals, radiation patterns and maximum intensities are set according to the above sections.

The simulation setup described above was run 200 times with all active whales randomly repositioned with 1000 m minimal inter-individual separation and the silent whale being 1000 m away from the buoy. This amounts to a total of 1600 simulations, each calculating the resulting signals at the buoy stemming from one vocal and one silent whale. For each click produced in a simulation the following information is stored: whale position (vocal and silent), on-axis click sound pressure level, piston model diameter, environmental conditions (wave height, reflection ratio at the bottom, ambient noise level and type), ray angular tolerance, azimuth and elevation of the whale, levels, bearings and delays of the reverberated clicks arriving at the buoy. Software configuration of some basic parameters prior to simulations is presented in Table 1.

Every click produced by a single whale creates 12 paths of measurable arrival levels at the buoy (see Figure 5): three from its source to the buoy (direct, surface- and bottom-reflected); three to the silent whale, each producing another three paths to the buoy. Consequently, the signal at the buoy is altered by the silent whale 9 times.

RESULTS

Figure 6 shows the distribution of the received levels at the buoy from rays reflected by the silent whale. The number of echoes represents those received out of the 72 reflected rays (8 clicks create 3 paths to the silent whale, each resulting in another 3 paths to the buoy) for each scenario. Signal level distribution is centred on sea-state 1 background noise level (1–30 kHz) with a right-hand side tail decreasing until sea-state 3 background noise level.

As sea-states are rarely below 2, especially in the Canary Islands, a first conclusion is that techniques to increase the SNR must be applied to ensure reasonable detection rates. These techniques could build upon the following observations:

1. The fact that clicks are to be repeated on an average of 1 click per second and per whale, implies that the silent whale is likely to be illuminated at least at this rate, and in the rather conservative case that only one whale is a contributing source. Integrated on a 10 s window, the coherent addition of the silent responses are to increase the SNR by at least 10 dB.
2. A beam-formed phased array would increase the SNR, with the additional benefit of resolving bearing information of the silent whale. Moreover, the broadband nature of the signals of interest here permits the use of sparse arrays of high directionality because frequency-specific grating lobes do not add up coherently in space. This technical scenario was simulated with *Songlines*. A 4 m-diameter ring array of 32 omni-directional hydrophones was beam-formed in the time-domain on one typical scenario, under the same control parameters as above. The silent whale was positioned 100 m deep and 1500 m away from the antenna. The software

https://doi.org/10.1017/S0025315407054951 Published online by Cambridge University Press

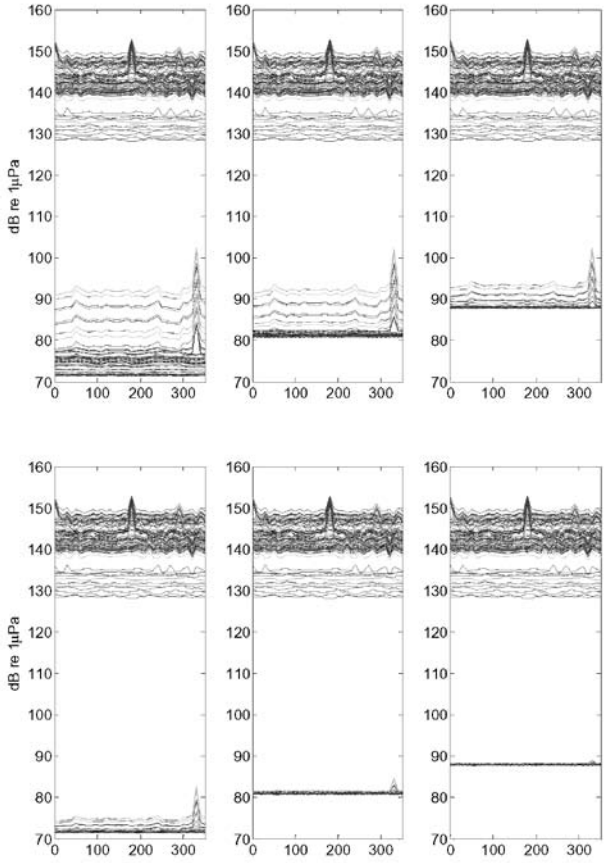

Figure 7. Received levels on the 32 time-based beam-formed beams of a Ø4m-32-sensor-antenna for sea state 1, 3 and 6 (left to right) and three passive-active whale types of orientation: from top to bottom: whale angle of view is near beam aspect, and tail-aspect (see text). Array DI is 12 dB (see text).The simulated silent whale is at 330° azimuth, 100 m depth, 1100 m horizontal distance from the buoy. The cumulated plot results from a 25 s period with 8 whales clicking at depth (see text). Total number of clicks was 189. Beams are altered by the direct and reverberated paths from the vocal whales' clicks directly to the buoy (90 dB and over).

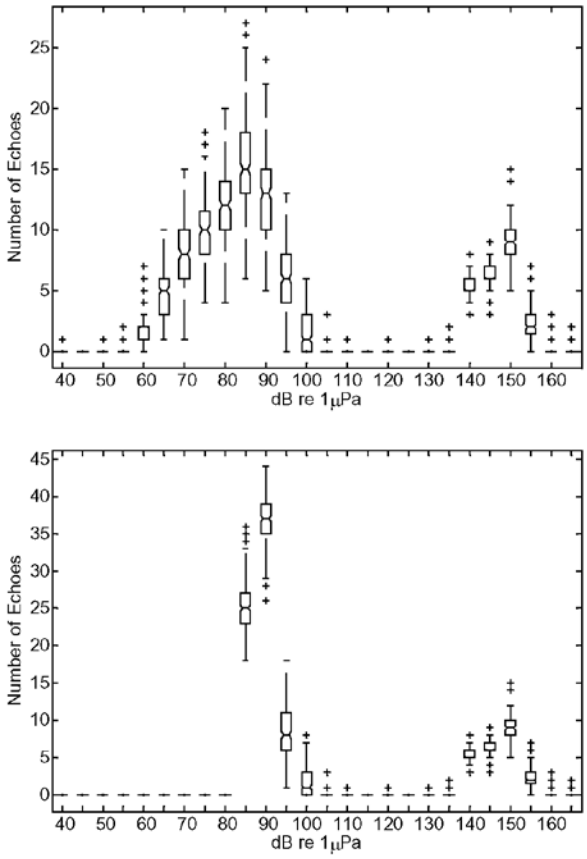

Figure 8. Distribution of direct, surface, bottom-reflected and silent-whale reverberated clicks. The top figure is the level-expanded version of Figure 6, which highlights the bimodal aspect of the received level distribution. The bottom figure represents the resulting distribution at sea-state 1 with an omni-directional receiver. The same results are obtained on one beam for sea-state 3 after beam-forming with the antenna described in the text.

also allowed to recreate the full waveforms resulting from the multi-path propagation of clicks to the buoy. Each whale produced a click at a random ICI taken from a uniform distribution in the 0.5–1 s interval during a 25 s period. Whales were separated by at least 1 km and repositioned every 5 s according to a group horizontal speed of 2 knots. The rest of the simulation settings remained unchanged. Results are presented in Figure 7.

3. Matched filtering using pre-localized sources could raise the SNR in cases when sea-state and the resulting greater noise levels and reverberations alter the detection rates. However, as clicks are highly directional, matched filtering in the case of sperm whales may not always perform as expected as both source signal and reverberated replicas tend to differ when the source heading changes. As seen in the previous section on click time–frequency characteristics, both time and frequency contents are angle-dependent. As this angle is random to the receiver in most cases, the hypothesis of a deterministic signal is not fulfilled and thus matched filtering would not be optimal (Bouvet, 1992). It is also likely that matched filtering would be less efficient at greater ranges, where signals are more distorted. According to Daziens (2004), sperm whale clicks matched filtering was indeed outperformed by an energy detector for ranges greater than 3000 m. In fact, the latter outperformed matched filtering only for sperm whale click detection. Detection ranges were then nearly doubled as compared to matched filtering, for the same source level, detection and false-alarm probabilities, of 50% and 1% respectively. In our case, as the two-way propagation (source to silent whale to receiver) results in greater attenuation and distortion than those resulting from a one-way propagation of the same distance, it is expected that the energy detector will outperform matched filtering.

4. In view of the above, which advises a simplistic pre-processing method based on beam-forming and signal energy, we plotted the received signal intensity distributions from 25 ms time-intervals in Figure 6 (no background noise, no beam-forming) and Figure 8 (with background noise and beam-forming). Figure 6 shows that the resulting probability density function is bimodal, where the low-level mode represents the click energy reverberated from the silent whale, and the high-level mode, centred above 120 dB, stems

https://doi.org/10.1017/S0025315407054951 Published online by Cambridge University Press

from the click direct, surface and bottom reflected energy at the receiver. We anticipate that simultaneous occurrence of these two modes on a limited number of beams could prove robust for a decision stage.

DISCUSSION

For a given and well characterized signal, detection probabilities mostly depend on the background noise level. Before attempting the implementation of our passive approach in a specific area, it should be noted that ambient noise level statistics are the most limiting factor. We inferred from the literature that, in the band of interest, noise level was around 90 dB_{rms} *re* 1μPa for sea-state 1 and a 1–30 kHz bandwidth. From our simulation results, energy-based detection thresholds would work until 1000 m. Nonetheless, each increase of 6 dB in background noise level, which is far from unusual, would half the detection range, as most propagation spreading is spherical in our case, and would make the system unreliable due to the dependency on weather conditions.

Advanced post-processing of the received low-level signals was not studied. The inherent spatio-temporal nature of sperm whale acoustics and behaviour requires the use of either stochastic or determinist signal processing to further increase the SNR. Statistical methods for ANI have been thoroughly studied in shallow water (Potter & Chitre, 1996, 1999), but due to the numerous contextual differences, especially the limited number of active sources, it is likely that a stochastic approach would not be appropriate in our case. On the other hand, a determinist approach founded on proper modelling of source angular variability could prove robust. Among other well documented methods, passive 3D localization of active sperm whales could then provide triggering information to coherently sum up the silent whale's response and increase the SNR and compensate for the ambient noise variability.

The reported multi-pulse structure of (most probably) off-axis clicks was not simulated, due to our incapacity to infer a model of its three-dimensional properties. We hence limited our study to the propagation of the first main pulse. Yet, including this feature would not impact upon the received levels except in the rare cases of constructive or destructive overlaps. The greatest impact would more likely be on the 'fill-up' of the time–space window with more high-energy pulses at the monitoring point, which may handicap the search for low level echoes in background noise. It is generally reported that the secondary pulses are rarely more than two or three and only appear at frequencies higher than 4 to 5 kHz (see Figure 1). The whole signal duration may then increase to 20 msec which results in a maximum 20×8×2=320 msec time period. This is one-third of the search time window, for 8 vocal whales and taking direct, surface and bottom reflected signals to the buoy into account, at a rate of 1click/whale/s. In the usual case, detection rates would not be drastically altered.

This paper would not be complete without a note on false alarm rates and how they would impact on a vessel's decision, as detectable echoes from the surface may often come from different sources, like a densely concentrated group of fish. At-sea experiments and real recordings may provide the relevant information to discriminate these other types of objects, e.g. by incorporating their monitored spatio-temporal and behavioural characteristics.

Scattering was only modelled by surface and bottom reflection coefficients being altered depending on sea-state and bottom type, respectively. As a result, our scattering model only affects specular rays. Reverberation, e.g. non-specular rays back-scattered from surface, bottom or deep scattering layers was not mentioned nor simulated. When propagating through a deep scattering layer, direct rays from source to target could also reach the receiver with interference scattered from the deep layer, attenuated by 40 to 50 dB (Jensen et al., 2000). Such attenuation could differ when deep scattering layers are at lower depth at night time. During day time, such layers tend to be at greater depths and would be further attenuated due to propagation loss. In either case, the resulting reverberations may interfere with the low-level echoes from silent whales. Similarly, modelling of surface and bottom scattering would provide important information on the interferences from the reverberated sources as a function of sea-state and time, since no detection will be possible if these are omnipresent, even for low scattering strengths. Even though we have shown that signals echoed from silent whales could be detectable at only low sea-states, when surface scattering may become negligible, bottom scattering strength could constantly interfere with and increase noise to critical levels.

In this work, simulations accounted for a given number of vocalizing whales, each producing one direct, one surface-reflected and one bottom-reflected ray to the receiver and to one silent whale, which in turn radiated the corresponding echoes modelled by one direct, one surface-reflected and one bottom-reflected ray to the receiver. In fact, these 12 resulting rays represent only one part of the real signal at the receiver, as all vocalizing whales would also scatter energy from other whales' clicks. In addition, simulations were limited to allow only one bottom and one surface reflection. Multiple reflections from vocalizing whales' clicks would originate weak signals of a similar order of magnitude as the simulated silent whale's echoes and should be discarded as well. So far, we have not studied how adding these additional scatterers and pathways could alter the current results, as the objective of this work was to study whether a signal excess from a silent whale near the surface could be measured. The raised ambiguity and false-alarm rates due to unpredicted and more complex pathways would probably call for a more advanced detector. As the primary task of the WACS is to localize active whales using an array of receivers, the resulting information could be used to perform forward modelling of the arrival structure, and then to compare this with observations to identify the anticipated replica arrivals. Echoed signals from silent whales could then be detected by a band-limited energy detector. In future work the authors hope to be able to simulate the same scenario with an unlimited number of reflections and enable back-scattering from active whales so that more complex detectors and matched field methods can properly be evaluated.

While this study is restricted to sperm whales, the ANI approach might progressively extend to wider possibilities, as large baleen whales passing through a wide pod of sperm

https://doi.org/10.1017/S0025315407054951 Published online by Cambridge University Press

whales are also to be detected, probably with higher contrast in the case of species such as fin and blue whales. Most large baleen whales only produce very low frequency sounds (most of the energy remains below 100 Hz) that reverberate in a complex way in the SOFAR channel and mix with all types of low-frequency sources summing up to great sound pressure levels (Potter & Delory, 1998; Stafford et al., 1998; Chiu et al., 1999). As a direct consequence, designing a permanent solution for passive localization of these whales is a difficult task and furthermore can be performed only with very wide aperture bottom-mounted arrays (Abileah, 1996; Chiu et al., 1999; Andrew et al., 2002). The low and, at times, negative signal-to-noise ratios at relatively short range from the whales have motivated the specific development of advanced signal processing algorithms that have not yet been implemented and still need further development (Delory & Potter, 1999; Delory et al., 1999). We believe that our approach could be an alternative worth considering in areas where sperm whale populations are geographically dense and stable over time. Furthermore, this method would have to be a complementary component of a more complex system like the previously described WACS in order to be viable and useful.

In conclusion, the results provide quantitative information as regards the implementation of a passive approach using sperm whale clicks as illuminating sources. Received levels are centred on ambient noise levels for low sea-states, motivating the use of beam-forming to raise signal levels and extract bearing information. Validation of the method introduced in this paper is essential before advanced signal enhancement techniques can be properly evaluated, leading to the prior necessity of performing experiments in the field. From a broader perspective, as permanent passive techniques based on natural acoustic energy would be probably less costly and less prejudicial to cetaceans than conventional active solutions the authors believe that they merit further investigation.

We are grateful to J.R. Potter, Acoustic Research Laboratory, National University of Singapore, who encouraged the use of ANI, following M. André's suggestions to apply it for the prevention of ship–whale collisions. We thank B. Møhl and his team at the University of Aarhus (Denmark), for providing the near on-axis click we used in our simulations, S. Krastel, University of Bremen (Germany), for the high-resolution bathymetry, along with Angeles Marrero and Pablo Sangra at the University of Las Palmas de Gran Canaria (Spain) for the water temperature and salinity data from the Canary Islands. We thank Manell Zakharia from the Ecole Navale (France) for pointing out an error in the noise levels. We also thank David Shea, from the University of Las Palmas de Gran Canaria for revising the English.

REFERENCES

Abileah, R.M., Lewis, S.D. & Gisiner, B., 1996. Long-range acoustic detection and tracking of the humpback whale Hawaii–Alaska migration. *Oceans'96 MTS/IEEE Proceedings*, pp. 373–377.

Alder-Frenchel, H.S., 1980. Acoustically derived estimate of the size distribution for a sample of sperm whales, *Physeter catodon*, in the western north Atlantic. *Canadian Journal of Fisheries and Aquatic Sciences*, **37**, 2358–2361.

André, M., 1997. *El cachalote*, Physeter macrocephalus, *en las Islas Canarias*. PhD Thesis. Universidad de Las Palmas de Gran Canaria.

André, M. & Kamminga, C., 2000. Rhythmic dimension in the echolocation click trains of sperm whales: a possible function of identification and communication. *Journal of the Marine Biological Association of the United Kingdom*, **80**, 163–169.

André, M., Delory, E. & van der Schaar, M., 2004a. *A passive acoustic solution to 3D whale monitoring*. Brest, France: Sea-Tech Week.

André, M., Delory, E. & van der Schaar, M., 2004b. *A passive mitigation solution to the effects of human-generated sound on marine mammals*. London: Policy on Sounds and Marine Mammals: an International Workshop.

André, M., Delory, E., van der Schaar, M. & Castell, J.V., 2005. *On the possibility of detecting and tracking echolocating whales by passive acoustics and ambient noise imaging*. La Rochelle, France: Workshop on Active Sonar, 19th Conference of the European Cetacean Society.

Andrew, R.K., Howe, B.M. & Mercer, J.A., 2002. Ocean ambient sound: comparing the 1960s with the 1990s for a receiver off the California coast. *Acoustic Research Letters Online*, **3**, 65–71.

Aroyan, J.L., 1996. *Three-dimensional numerical simulation of biosonar signal emission and reception in the common dolphin*. PhD. University of California, Santa Cruz.

Au, W.W.L. & Herzing, D.L., 1997. Measurement of the echo location signals of the Atlantic spotted dolphin *Stenella frontalis* in the waters off the Grand Bahamas. *Journal of the Acoustical Society of America*, **101**, 3137–3138.

Au, W.W.L. & Herzing, D.L., 2003. Echolocation signals of wild Atlantic spotted dolphin (*Stenella frontalis*). *Journal of the Acoustical Society of America*, **113**, 598–604.

Au, W.W.L., Moore, P.W.B. & Pawlowski, D., 1986. Echolocation transmitting beam of the Atlantic bottlenose dolphin. *Journal of the Acoustical Society of America*, **80**, 688–691.

Beedholm, K. & Mohl, B., 2006. Directionality of sperm whale sonar clicks and its relation to piston radiation theory. *Journal of the Acoustical Society of America*, **119**, EL14–EL19.

Best, P., 1979. Social organization in sperm whales, *Physeter macrocephalus*. In *Behaviour of marine animals* (ed. H.E. Winn and B.L. Olla), pp. 227–289. New York, London: Plenum Press.

Bouvet, M., 1992. *Traitement des signaux pour les systèmes sonar*. Masson: CNET-ENST.

Buckingham, M.J., Potter, J.R. & Epifanio, C.L., 1996. Seeing underwater with background noise. *Scientific American*, **274**, 40–44.

Caldwell, D.K., Caldwell, M.C. & Rice, D.W., 1966. Behavior of the sperm whale, *Physeter macrocephalus*. In *Whales, dolphins and porpoises* (ed. K.S. Norris), pp. 677–717. Berkeley: University of California Press.

Chiu, C.-S., Miller, C.W., Moore, T.C. & Collins, C.A., 1999. Auto-detection and censusing of blue whale vocalizations along the central California Coast using a bottom-lying hydrophone array. *Proceedings of the Oceanology International '99 Pacific Rim Conference*, 435–440.

Cranford, T.W., 1999. The sperm whale's nose: sexual selection on a grand scale? *Marine Mammal Science*, **15**, 1133–1157.

Daziens, J.M., 2004. *Assessing the performance of omni-directional receivers for passive acoustic detection of vocalizing odontocetes*. Monterey, California: Naval Postgraduate School.

Delory, E. & Potter, J.R., 1999. Transient, tonal, and background noise filtering with wavelet and cosine transforms. *Journal of the Acoustical Society of America*, **105**, 1106.

Delory, E., Potter, J.R., Miller, C. & Chiu, C.-S., 1999. *Detection of blue whales A and B calls in the northeast Pacific Ocean using a multi-scale discriminant operator*. Maui, Hawaii: 13th Biennial Conference on the Biology of Marine Mammals.

Douglas, L.A., Dawson, S.M. & Jaquet, N., 2005. Click rates and silences of sperm whales at Kaikoura, New Zealand. *Journal of the Acoustical Society of America*, **118**, 523–529.

Dunn, J.L., 1969. Airborne measurements of the acoustic characteristics of a sperm whale. *Journal of the Acoustical Society of America*, **46**, 1052–1054.

Etter, P.C., 2003. *Underwater acoustic modeling. Principles, techniques and applications*. London: Spon Press.

Finneran, J.J., 2003. Whole-lung resonance in a bottlenose dolphin (*Tursiops truncatus*) and white whale (*Delphinapterus leucas*). *Journal of the Acoustical Society of America*, **114**, 529–535.

Goold, J.C., 1996. Signal processing techniques for acoustic measurement of sperm whale body lengths. *Journal of the Acoustical Society of America*, **100**, 3431–3441.

Goold, J.C. & Jones, S.E., 1995. Time and frequency domain characteristics of sperm whale clicks. *Journal of the Acoustical Society of America*, **98**, 1279–1291.

Gordon, J., 1987. Sperm whale groups and social behaviour observed off Sri Lanka. *Reports of the International Whaling Commission*, **35**, 205–217.

Gordon, J.C.D., 1991. Evaluation of a method for determining the length of sperm whales, *Physeter catodon*, from their vocalisations. *Journal of Zoology*, **224**, 301–314.

Gordon, J. & Steiner, L., 1992. Ventilation and dive patterns in sperm whales, *Physeter macrocephalus*, in the Azores. *Reports of the International Whaling Commission*, **42**, 561–565.

Jaquet, N. & Whitehead, H., 1996. Scale-dependent correlation of sperm whale distribution with environmental features and productivity in the South Pacific. *Marine Ecology Progress Series*, **135**, 1–9.

Jaquet, N., 1996. How spatial and temporal scales influence understanding of sperm whale distribution: A review. *Mammal Review*, **26**, 51–65.

Jaquet, N., Dawson, S. & Douglas, L., 2001. Vocal behavior of male sperm whales: why do they click? *Journal of the Acoustical Society of America*, **109**, 2254–2259.

Jefferson, T.A., Leatherwood, S. & Webber, M.A., 1993. *Marine mammals of the world*. FAO Species Identification Guide. Food and Agriculture Organization of the United Nations.

Jensen, F.B., Kuperman, W.A., Porter, M.B. & Schmidt, H., 2000. *Computational Ocean Acoustics*. New York: Springer-Verlag.

Krastel, S. & Schmincke, H.U., 2002. The channel between Gran Canaria and Tenerife: constructive processes and destructive events during the evolution of volcanic islands. *International Journal of Earth Sciences*, **91**, 629–641.

Levenson, C., 1974. Source level and bistatic target strength of the sperm whale (*Physeter catodon*) measured from an oceanographic aircraft. *Journal of the Acoustical Society of America*, **55**, 1100–1103.

Love, R.H., 1973. Target strengths of humpback whales *Megaptera novaeangliae*. *Journal of the Acoustical Society of America*, **54**, 1312–1315.

Mackenzie, K.V., 1981. 9-term equation for sound speed in the oceans. *Journal of the Acoustical Society of America*, **70**, 807–812.

Makris, N.C. & Cato, D.H., 1994. Using singing whales to track nonsingers. *Journal of the Acoustical Society of America*, **96**, 3270.

Makris, N.C., Lai, Y.-S. & Cato, D.H., 1999. Using broadband humpback whale vocalizations to locate nonvocal whales in shallow water. *Journal of the Acoustical Society of America*, **105**, 993.

Miller, J.H. & Potter, D.C., 2001. *Active high frequency phased-array sonar for whale shipstrike avoidance: target strength measurements*. Honolulu, HI, USA. OCEANS, 2001. MTS/IEEE Conference and Exhibition, pp. 2104–2107.

Miller, J.H., Weber, T. & Tuttle, A., 1999a. The dependence of target strength of the northern right whale (*Eubalaena glacialis*) on the acoustic properties of blubber. *Journal of the Acoustical Society of America*, **106**, 2163.

Miller, J.H., Potter, D.C., Weber, T. & Felix, J., 1999b. The target strength of the northern right whale (*Eubalaena glacialis*). *Journal of the Acoustical Society of America*, **105**, 992.

Møhl, B. & Amundin, M., 1991. Sperm whale clicks: pulse interval in clicks from a 21m specimen. In *Sound production in odontocetes, with emphasis on the harbour porpoise*, Phocoena phocoena. (PhD thesis by Amundin, M.) University of Stockholm, pp 115–125.

Møhl, B., Larsen, E. & Amundin, M., 1981. *Sperm whale size determination: outlines of an acoustic approach*. FAO Fisheries Series. 5, 327–332.

Møhl, B., Wahlberg, M., Madsen, P.T., Miller, L.A. & Surlykke, A., 2000. Sperm whale clicks: directionality and source level revisited. *Journal of the Acoustical Society of America*, **107**, 638–648.

Møhl, B., Wahlberg, M., Madsen, P.T., Heerfordt, A. & Lund, A., 2003. The monopulsed nature of sperm whale clicks. *Journal of the Acoustical Society of America*, **114**, 1143–1154.

Nishiwaki, M., Ohsumi, S. & Maeda, Y., 1963. Change of form in the sperm whale accompanied with growth. *Scientific Reports of the Whales Research Institute, Tokyo*, **17**, 1–13.

Norris, K.S. & Harvey, G.W., 1972. A theory for the function of the spermaceti organ of the sperm whale (*Physeter catodon* L.). In *Animal orientation and navigation* (ed. S.R. Galler et al.), pp. 397–417. Washington, D.C: NASA.

Pallayil, V., Chitre, M.A., Tan, E.T., Potter, J.R., Koay, T.B., Ruiz, S.B. & Tan, S.P., 2003. *Ambient noise imaging—first deployments of ROMANIS and preliminary data analysis*. San Diego, USA. Oceans 2003 Marine Technology and Ocean Science Conference (MTS/IEEE).

Pavan, G., Hayward, T.J., Borsani, J.F., Priano, M., Manghi, M., Fossati, C. & Gordon, J., 2000. Time patterns of sperm whale codas recorded in the Mediterranean Sea 1985–1996. *Journal of the Acoustical Society of America*, **107**, 3487–3495.

Philips, J.D., Nachtigall, P.E., Au, W.W.L., Pawloski, J.L. & Roitblat, H.L., 2003. Echolocation in the Risso's dolphin, *Grampus griseus*. *Journal of the Acoustical Society of America*, **113**, 605–616.

Potter, J.R. & Chitre, M., 1996. Statistical models for ambient noise imaging in temperate and tropical waters. *Journal of the Acoustical Society of America*, **100**, 2738–2739.

Potter, J.R. & Chitre, M., 1999. Ambient noise imaging in warm shallow seas; second-order moment and model-based imaging algorithms. *Journal of the Acoustical Society of America*, **106**, 3201–3210.

Potter, J.R. & Delory, E., 1998. *Noise sources in the sea and the impact for those who live there*. Singapore: Acoustic and Vibration, Asia' 98.

Potter, J.R., Buckingham, M.J., Deane, G.B., Epifanio, C.L. & Carbone, N.M., 1994. Acoustic daylight: preliminary results from an ambient noise imaging system. *Journal of the Acoustical Society of America*, **96**, 3235.

Rasmussen, M.H., Miller, L.A. & Au, W.W.L., 2002. Source levels of clicks from free-ranging white-beaked dolphins (*Lagenorhynchus albirostris* Gray 1846) recorded in Icelandic waters. *Journal of the Acoustical Society of America*, **111**, 1122–1125.

Richardson, W.J., Greene, C.R., Malme, C.I. & Thomson, D.H., 1995. *Marine mammals and noise*. San Diego: Academic Press.

Stafford, K.M., Fox, C.G. & Clark, D.S., 1998. Long-range acoustic detection and localization of blue whale calls in the northeast Pacific Ocean. *Journal of the Acoustical Society of America*, **106**, 3616–3625.

Tucker, D.G. & Glazey, B.K., 1966. *Applied underwater acoustics*. London: Pergamon Press Ltd.

Urick, R.J., 1996. *Principles of Underwater Sound*. Slough, UK: Peninsula Publishing.

Watkins, W.A., 1980. Sperm whale clicks. In *Animal sonar systems* (ed. R.-G. Busnel and J.F. Fish), pp. 283–290. New York: Plenum.

Watkins, W.A. & Schevill, W.E., 1977. Sperm Whale Codas. *Journal of the Acoustical Society of America*, **62**, 1485–1490.

Watwood, S.L., Miller, P.J.O., Johnson, M., Madsen, P.T. & Tyack, P.L., 2006. Deep-diving foraging behaviour of sperm whales (*Physeter macrocephalus*). *Journal of Animal Ecology*, **75**, 814–825.

Weilgart, L. & Whitehead, H., 1993. Coda communication by sperm whales (*Physeter macrocephalus*) off the Galapagos Islands. *Canadian Journal of Zoology*, **71**, 744–752.

Weilgart, L.S. & Whitehead, H., 1988. Distinctive vocalizations from mature male sperm whales (*Physeter macrocephalus*). *Canadian Journal of Zoology*, **66**, 1931–1937.

Whitehead, H. & Weilgart, L., 1990. Click rates from sperm whales. *Journal of the Acoustical Society of America*, **87**, 1798–1806.

Zimmer, W.M.X., Johnson, M.P., D'Amico, A. & Tyack, P.L., 2003. Combining data from a multisensor tag and passive sonar to determine the diving behavior of a sperm whale (*Physeter macrocephalus*). *IEEE Journal of Oceanic Engineering*, **28**, 13–28.

Zimmer, W.M.X., Tyack, P.L., Johnson, M.P. & Madsen, P.T., 2005a. Three-dimensional beam pattern of regular sperm whale clicks confirms bent-horn hypothesis. *Journal of the Acoustical Society of America*, **117**, 1473–1485.

Zimmer, W.M.X., Madsen, P.T., Teloni, V., Johnson, M.P. & Tyack, P.L., 2005b. Off-axis effects on the multipulse structure of sperm whale usual clicks with implications for sound production. *Journal of the Acoustical Society of America*, **118**, 3337–3345.

Submitted 16 June 2006. Accepted 20 November 2006.